

## Impingement Cooling Characteristics of a Cube in Cross Flow

Jalal M. Jalil  , Sabah T. Ahmed \*\* & Adnan A. Abdel Rasool\*\*

Received on: 29/9/2008

Accepted on: 13/11/2008

### Abstract

An experimental and numerical investigation is carried out for the heat transfer from a cube faces subjected to impinging jet which centrally strikes the top face of the cube. The cube is subjected also to a comparatively low velocity cross flow through the duct occupying the cube. Different factors affecting the cooling characteristics of the cube are studied as orifice size, jet velocity and orifice to cube top distance. The results show that cross flow increases heat rates from the cube for small size orifices and low impinging jet velocities. Orifice sizes equal or bigger than cube size will isolate the cube from cross flow effect especially at high impinging jet velocities.

### مميزات التبريد التصادمي للجريان عبر مكعب

#### الخلاصة

أجريت دراسة عملية و نظرية لانتقال الحرارة من اوجه مكعب معرض لنفث موجه الى الوجه العلوي للمكعب. المكعب معرض كذلك لجريان جانبي ذو سرعة قليلة نسبيا خلال المجرى الذي يحوي المكعب. لقد درست العوامل المؤثرة على عملية التبريد مثل حجم المنفتح، سرعة المنفتح والمسافة العمودية بين المنفتح والمكعب. اظهرت النتائج ان الجريان الجانبي يزيد انتقال الحرارة من المكعب لاجسام المنفتح الصغيرة ولسرع المنفتح الصغيرة. احجام المنفتح التي تساوي او التي اكبر من حجم المكعب سوف تعزل المكعب عن الجريان الجانبي و خاصة لسرع النفث العالية.

### Nomenclature

$C_1, C_2, C_M, C_D$	Coefficients in dissipation equation
$E_c$	Log law constant
$H$	Duct height mm
$H_o$	Distance from orifice to cube top face mm
$h$	Local height transfer coefficient $W/m^2 K$
$h_{av}$	Average heat transfer coefficient $W/m^2 K$
$k$	Kinetic energy
$L$	Cube side length mm
$Nu]_{C,F}$	Average Nusselt number for the cube in case of impingement with cross flow = $\frac{h_{avx}L}{k_f}$
$Nu]_{D,F}$	Average Nusselt number for the cube in case of duct flow only i.e. $U_j = 0.0, Nu]_{D,F} = \frac{h_{avx}L}{k_f}$

\* Electromechanical Engineering Department University of Technology/Baghdad

\*\* Mechanical Eng. Dept. University of Technology/Baghdad

$k_f$	Conductivity of air W/m K
$Re_L$	Reynolds number based on air jet velocity, $Re_L = \frac{U_j L}{\nu_{air}}$
$\nu_{air}$	Kinematic viscosity of air

## Introduction

Impingement cooling is widely used in different industrial processes as glass manufacturing paper drying, electronics cooling. Impinging jet of air usually gives a heat transfer rates which is higher than commonly used duct air flows. The impinging cooling of electronic modules is modeled by the impingement of an air jet which strikes orthogonally the top face of the module and flows in a horizontal direction towards the duct exit. In case of multi jet impingement the flow in the horizontal direction accumulates forming a horizontal cross flow, which is usually at lower velocities compared to the impinging air jet velocities. Fig. 1 shows the physical geometry usually used in the actual practice in industrial applications. Impingement cooling of a surface has been extensively studied by different authors and different factors affecting the efficiency of cooling process of a surface are verified. The main factors are the orifice to surface distance, jet velocity, orifice size, cross flow velocity. Research works concerned with impingement cooling of a three dimensional object are rare. This work verify the cooling characteristics of a cube which simulates an electronic module placed at a central position of a duct and subjected to both impingement and cross flow. Local temperature distribution on cube faces is measured and local heat transfer coefficients are then calculated from it. Average heat transfer coefficient for the whole cube is then calculated and different factors affecting the cooling behaviour of the cube are then discussed. CFD based on finite volume method are used to analyze the flow field and heat transfer rates from cube faces and comparison with available experimental data is carried out.

Two types of air flow are considered in this research, impingement flow conjugated with common air duct flow referred to as a cross flow. Different research works considered each type separately.

Anderson, et al. [1] discussed forced convection heat transfer in a channel populated with discrete component. The temperature rise of each component is expressed as the sum of two parts, its adiabatic temperature rise, due to the thermal wakes of upstream component, and its self heating temperature rise. Mienders, et al. [2] presented the results of experimental investigation of local convective heat transfer from wall mounted single array of cubical protrusion along a wall of a wind tunnel. The results showed a high non-uniformity of the local convective heat transfer over the surfaces of the individual elements. Mienders, et al. [3] presented the experimental results from configurations of wall mounted cubes in a channel flow. From flow analysis it appeared that the flow structure around the protruding cubes is characterized by flow separation, reattachment and recirculation which dictate the local convective heat transfer phenomenal significantly. Mienders [4] presented the results of experimental investigation of the local convective heat transfer on a wall-mounted cube placed in a developing turbulent channel flow for  $2750 < Re_H < 4970$ . Experiments were conducted using an especially design cube assembly made of heated copper core and a thin epoxy layer on its surface. The flow field is studied by laser Doppler anemometer and flow visualizations. Maximum coefficients are located at points of reattachment while minimum

coefficients are at recirculation zone caused by trapped vortex. Hansen, et al. [5] performed experiments to characterize heat transfer to a normally impinging air jet from surfaces modified with arrays of fin-type extension. For modified surfaces the system effectiveness decreased monotonically with increasing nozzle to plate distance in contrast to the smooth surface behaviour. Hollworth, et al. [6] conducted experiments to determine the performance of a system of low velocity air jets to cool a simulated electronics package. Each element was cooled by a cluster of four jets, and spent fluid was vented at one end of the channel formed between the circuit board and the plate from which the jets were discharged. The results show that the cross flows of the spent air appears to enhance heat transfer for those elements near the exit end of the channel. Tummers, et al. [7] reported a paper on the flow structure and surface temperature distribution of a heated wall-mounted cube from an in-line array, subjected to cooling by the combined action of channel flow and an impinging jet from constant diameter orifice. The local flow structure in terms of flow separation and reattachment, and the rolling up of separating shear layers, has marked influence on local temperature distribution on the surface of the cube. Rundstrom, et al. [8] used two different turbulence models ( $\nu^2 - f$ ) and a Reynolds-stress model (RSM) with a two layer model in the near wall region, to analyze the flow around a cube placed in the central position of the base plate of a duct and subjected to both axial cross flow and impinging jet from above. The flow structure is highly complex. The main difference between the models is that the RSM produces a higher level of turbulent kinetic energy ( $k$ ) than the  $\nu^2 - f$  model in all regions and the largest differences are in the stagnation region at the top of the cube. Rundstrom, et al. [9] investigated an impinging jet in combination with low velocity channel flow on a cube using (RSM) turbulence

model. The geometrical case is a channel with a heated cube in the middle of the base plate and two inlets, one horizontal channel flow and one vertical impinging jet orifice diameter of 12mm and cube size length 15 mm. The effect of the jet Re and jet to cross velocity ratio are investigated. The air flow pattern around the cube and the surface temperature of the cube as well as the mean values and local distribution of heat transfer coefficients are presented.

### Experimental Setup

The apparatus shown in Fig. 2 and Plates 1,2 and 3 works in an open-coop airflow circuit which takes air from building and discharges it to the surrounding atmosphere. The air is drawn by the suction side of a blower 1.1 kW power through a control gate at blower intake, to adjust the amount of flow rate. The air is forced to flow through a circular PVC tube 150 mm in diameter, connected to a tee section reducer. The horizontal side of the tee section is connected to a bypass tube controlled by a valve, while the other 90° opening is connected to a pipe 100 mm in diameter with an orifice assembly is fitted at its other end. The orifice plate is made of Teflon and machined as disks with the orifice machined at its centre with the desired orifice size. The orifice plate is to be occupied centrally in the orifice assembly at the pipe end with an interference fit with a cap designed for this purpose. The pipe and orifice assembly is fixed to the top wall of a test section. Air flows through the orifice and impinges centrally normal to a cube fitted at the lower wall of the test section. The test section is made of plexiglass and has two ends at which airflow after impinging the cube. Additional two ducts, first works as intake duct with a bell mouth at its entrance and the second for discharging air from the other side. The discharging side is joined to the suction side of another blower, which draw air through the duct to the atmosphere. The test section and the two other ducts at intake and exhaust form one long duct which is mounted on a wooden

structure supported by a hydraulic jack. The supporting mechanism and lower side of the duct is designed in such a way that the relative position of the top face of the cube to the orifice plate fitted at the top wall of the duct is varied in predesigned displacements. The cube is made of a Plexiglas plate 3mm thick and its side length is 50 mm in dimension. The top face and one side face is drilled with 64 holes 0.5 mm in diameter so that a thermocouple type K junction 0.2 mm in diameter is inserted in each hole. The five faces (top and four sides) are engraved with 1mm undercut so that a wire heater 15  $\Omega/m$  resistance is inserted through the groove and then covered with five square aluminum plate having same cube side length and each plate is adhered to the cube face with a small drop of glue. The top and one of the side faces are drilled to occupy thermocouple junctions and are treated in the same way for other faces fitted with heater wire arrangement and precautions are taken so that the electrical heater is filled in the zone between the thermocouple holes. The inner portion of the cube made of Plexiglas sheet forms a cavity which is filled them with polyurethane foam as insulating material to reduce heat conducted from the outer faces to the inner portion of the cube. The cube is fitted at the central position of the lower plate of the test section which is made of Plexiglas and cut with a square opening having same size of the cube. Thermocouples are passed through this opening to a selector switch board used for temperature measurement of cube faces using digital thermometer type XMTA600 with error of  $\leq 0.5\%$ . Air jet velocities and cross flow velocities are controlled by the control valves and gates equipped with the test rig. Air jet velocities can be varied in the range 8-30 m/s with different sizes of orifice plates of 5 to 70 mm diameter.

Total tube fitted in a three dimensional traversing mechanism is used for air jet velocity distribution at orifice exit plane and at different axial positions in the direction of jet flow. Fig. 3 shows

velocity distribution for different orifice sizes and jet velocities. The figure reveals the standard behaviour and flow zones of the jet which are the potential zone characterized by constant velocity, the transition zone and the free zone. The large the orifice size the longer is the potential zone while small size orifice have shorter distance potential zone with orifice profile with a bell shaped velocity profile outward the potential zone and the bigger area covered by the impinging jet.

### Numerical Solution

The transport equations for continuity, momentum, energy, and the turbulence scales  $k$  and  $\epsilon$ , which all have the general form

$$\frac{\partial}{\partial x}(r_u f) + \frac{\partial}{\partial y}(r_v f) + \frac{\partial}{\partial z}(r_w f) = \frac{\partial}{\partial x}(\Gamma_f \frac{\partial f}{\partial x}) + \frac{\partial}{\partial y}(\Gamma_f \frac{\partial f}{\partial y}) + \frac{\partial}{\partial z}(\Gamma_f \frac{\partial f}{\partial z}) + S_f \dots (1)$$

Where  $\phi$  is the dependent variable and  $S_f$  is the source term. The convection and diffusion terms for all the transport equations are identical with  $\Gamma_f$  which represent the diffusion coefficient for scalar variables and the effective viscosity  $\mu_{eff}$  for vector variables. For solving the partial differential equations 1 for each variable, the control volume is divided into a number of control volumes; each volume is associated with particular dependent variable at a certain grid points. The scalar variables are stored at the main grid point while the velocity composites are stored at staggered grids. The differential equation is integrated over each control volume. The result is the discretisation equation containing the values of  $\phi$  for a group of grid points. The solution of this control volume formulation would imply that the integral conservation of quantities such as mass, momentum and energy is exactly satisfied over any group of control volumes and over the whole computation domain. The hybrid differencing scheme is

used for obtaining the discretisation equation for the three-dimensional based on the general differential equation 1. The simple algorithm by Patankar was applied. Fig. 4 shows the mesh used in the x-y plane, i.e., in the plane containing the length and the height of the duct respectively, while the other mesh constructed is for the y-z plane which represents the height and width of the duct respectively. The mesh number used is in the order of 60 x 30 x 30. The boundary conditions applied on cube surfaces are zero velocities (no slip conditions) and constant heat flux,  $q''$ . The outlet velocity of nozzle with circular outlet was approximated to rectangular mesh into the domain.

**Results**

The heat transfer rates are represented by the values of Nusselt number calculated on the basis of the average value of the heat transfer coefficient for the whole cube and the cube size L.

$$q'' = \frac{\text{heat transfer rate}}{\text{cube surface area}} = h(T_{\text{surface}} - T_{\text{bulk}}) \quad (2)$$

Fig. 5 represent the variation of Nusselt number  $[Nu]_{C,F}$  with  $Re_L$  at different orifice sizes of  $D = 5,10,20,30,40,50$  and  $70$  mm. Generally speaking the figures reveal that higher air jet velocities give linear rate of increase in Nusselt number. The higher the cross flow velocity (two cross flow velocities being tested are  $U_c=1.3$  and  $2.8$  m/s) give the higher value of  $Nu]_{C,F}$ . Notice the range  $Nu]_{C,F}$  values at different orifice sizes, shows that larger orifice sizes give higher  $Nu]_{C,F}$  values in the range of 20-30% except for  $D=70$  mm in which difference in  $Nu]_{C,F}$  values variation reduces to about 5-10%.

The  $Nu]_{C,F}/Nu]_{D,F}$  ratio calculated from experimental results is plotted versus  $Re_L$  values. The results are presented in Fig. 6 for orifice sizes of  $D=5,10,20,30,40,50$  and  $70$  mm for constant  $H/L$  value of 1.4 i.e., duct size is kept constant with  $Ho = 20$  mm. The general behaviour of  $[Nu]_{C,F}/[Nu]_{D,F}$  ratio

with  $Re_L$  shows a linear increase in  $Re_L$  with  $U_c = 2.8$  m/s ratios values is the smaller in comparison to  $U_c = 1.3$  m/s values reflecting higher values of  $[Nu]_{D,F}$  in case of  $U_c = 2.8$  m/s.

The  $[Nu]_{C,F}/[Nu]_L$  ratio which represent the ratio of Nusselt number average values in case of impingement with cross flow to the case of impingement only are plotted versus  $Re_L$  are shown in Fig. 7 corresponding to orifice diameters of  $D = 5,10,20,30,40,50$  and  $70$  mm.

The figure shows a gradual reduction in the values of the ratio with increasing value of  $Re_L$ . The values of the ratio are higher for the cross velocity  $U_c = 2.8$  m/s while the values of the ratio are smaller for the slower cross flow velocity  $U_c = 1.3$  m/s. The figures also declare that starting from the smallest size of the orifice  $D = 5$  mm, as the orifice size increases the range of the ratio  $[Nu]_{C,F}/Nu_L$  decreases from a value of 2.8 for  $D = 5$  mm at  $U_c = 2.8$  m/s and reaches a value less than unity for  $D = 70$  mm. The difference between the ratio values for the two cross velocities is noticed to be smaller as the orifice size increases. The conclusion from the above mentioned figures is that increasing the jet velocities of the impinging air will increase the heat transfer rates of the cube in a manner that the effect of the cross flow will be smaller in increasing the heat transfer, the larger the orifice size the smaller will be the effect of cross flow.

The numerical solution is used to find the flow field around the cube for two cross flow velocities  $U_c = 1.3$  and  $2.8$  m/s and for low and high jet velocities of  $U_j = 8$  and  $30$  m/s respectively. Fig. 8 shows the flow field around the cube for  $D = 70$  mm size orifice. The  $Z/L = 0.5$  section flow field shows the effect of the cross flow, a circulation flow is generated on the front face of the cube. On the rear face, the air washes up the face. The  $y/L = 0.1$  and  $y/L = 1.1$  sections of flow field show that the dominating flow just on the top face of the cube and upward its top face, is the cross flow velocity. Flow separation is

noticed on the front face of the cube and vortex generation is noticed on the rear face. The  $D = 10$  mm  $U_j = 30$  m/s,  $U_c = 1.3$  m/s results are shown in Fig. 9 which shows that the flow pattern is mainly a cross flow in characteristics and the impinging jet flow is limited to a small zone surrounding the jet impinging from the small size orifice in this case. Figure 10 shows comparison between numerical and experimental results of heat transfer coefficients on cube faces

and acceptable agreement was found in the percentage errors.

### Conclusions

1-The higher the cross flow the greater will be the heat transfer coefficients relative to case of impingement only. This is found true incase when the orifice size is small relative to the side length of the cube.

2-In case of big sizes of the orifice from which air impinges on the top of the cube, a blockage effect will reduce the average heat rates from the cube especially at high velocity of the impinging jet and the dominant effect in this case is the impinging jet effect.

3-Examining the flow field around the cube at different orifice sizes shows that the dominant effect at small orifice sizes is the cross flow effect except in regions above the cube, it is limited in its effect to small regions at which cross flow velocity turns around the impinging jet.

### References

- [1] A.M. Anderson and R.J. Moffat, "Direct Air Cooling of Electronic Components: Reducing Component temperatures by Controlled Thermal Mixing", Transacting of the ASME, Vol.113, PP.56-62, 1991.
- [2] E.R. Meinders, T.H. Vandermeer and K. Hanjalic, "Local Convective Heat Transfer from an Array of Wall Mounted Cubes", Int. Jr. Heat Mass Transfer, Vol.41, No.2, PP.335-346, 1998.
- [3] E.R. Meinders and K. Hanjalic, "Experimental Evaluation of the Local Convective Heat Transfer from Configurations of Wall-Mounted Cubes in a Channel Flow", Jr. of Electronics Cooling, Vol.4, No.1, PP.34-39, 1998.
- [4] E.R. Meinders, K. Hanjalic and R.J. Martinuzzi, "Experimental Study of the Local Convection Heat Transfer from a Wall Mounted Cube in Turbulent Channel Flow", Transaction of the ASME, Vol.121, PP.564-573, 1999.
- [5] L.G. Hansen and B.W. Webb, "Air Jet Impingement Heat Transfer from Modified Surfaces", Int. Jr. Heat Mass Transfer, Vol.36, No.4, PP.989-997, 1993.
- [6] B.R. Hollworth and M. Durbin, "Impingement Cooling of Electronics", ASME Jr. of Heat Transfer, Vol.114, PP.607-613, 1992.
- [7] M.J. Tummers, M.A. Filkweert, K. Hanjalic, R. Rodink and B. Moshfegh, "Impinging Jet Cooling of Wall Mounted Cubes", Accepted for Presentation at ERCOFTAC, International Symposium on Engineering Turbulence Modeling and Measurements-ETMM6, Sardinia, Italy, 23-25 May, 2005.
- [8] D. Rundstrom and B. Moshfegh, "Numerical Investigation of Flow Behaviour of an Impinging Jet in a Cross-Flow on a Wall Mounted Cube Using RSM and  $v^2$ -f Turbulence Models", 2004, [www.google.com](http://www.google.com), Keywords Impingement, Cube (Internet).
- [9] D. Rundstrom and B-Moshfegh, "Investigation of Flow and Heat Transfer of an Impinging Jet in a Cross Flow for Cooling of a Heated Cube", 2004, [www.google.com](http://www.google.com), Keywords Impingement, Cube (Internet).

**Table (1):** Comparison of experimental and numerical calculation results of average heat transfer coefficients on the cube faces in impingement with cross flow configuration.

cross flow  $H/L= 1.4$  ,  $D= 5$  mm

$U_j$	$U_c$	Top	side	front	rear
Exp.8m/sec	2.8	52.9	41.4	45	43.6
Num.		49.4	38.94	49.26	30.4
%error		6.6	6	9.4	43
Exp.8m/sec	1.3	42.8	32	36	25
Num.		52	42	55	22
%error		21	31	52	12

$D=20$  mm

$U_j$	$U_c$	Top	side	front	rear
Exp.8m/sec	2.8	54	45.7	42.2	42.7
Num.		44	40	49	27.9
%error		18	12.6	16.1	35
Exp.8m/sec	1.3	43.8	36.6	36	33.5
Num.		45	46	56	28
%error		3	25	35	22

$D=50$  mm

$U_j$	$U_c$	Top	side	front	rear
Exp.8m/sec	2.8	48.6	49	48.4	40.5
Num.		46	37	48	37
%error		5.3	24	0.5	8.6
Exp.8m/sec	1.3	41.6	37	41.8	34.8
Num.		41	38.3	46.7	37.7
%error		1.4	3.5	11	8.4

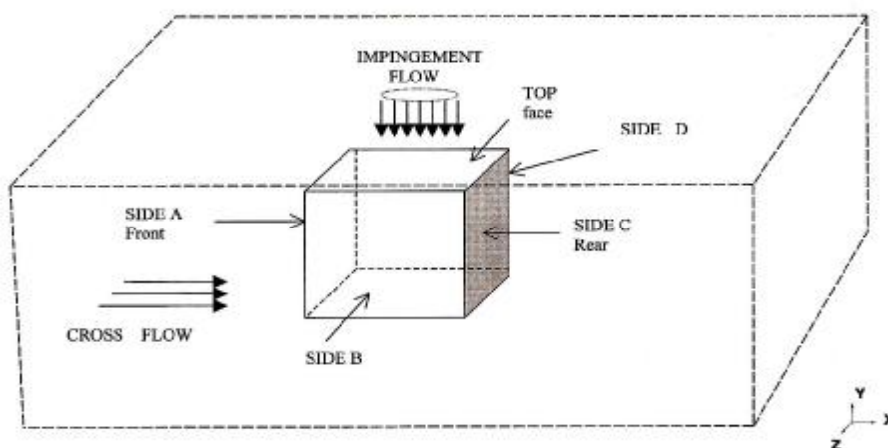


**Fig (1) Physical Geometry**

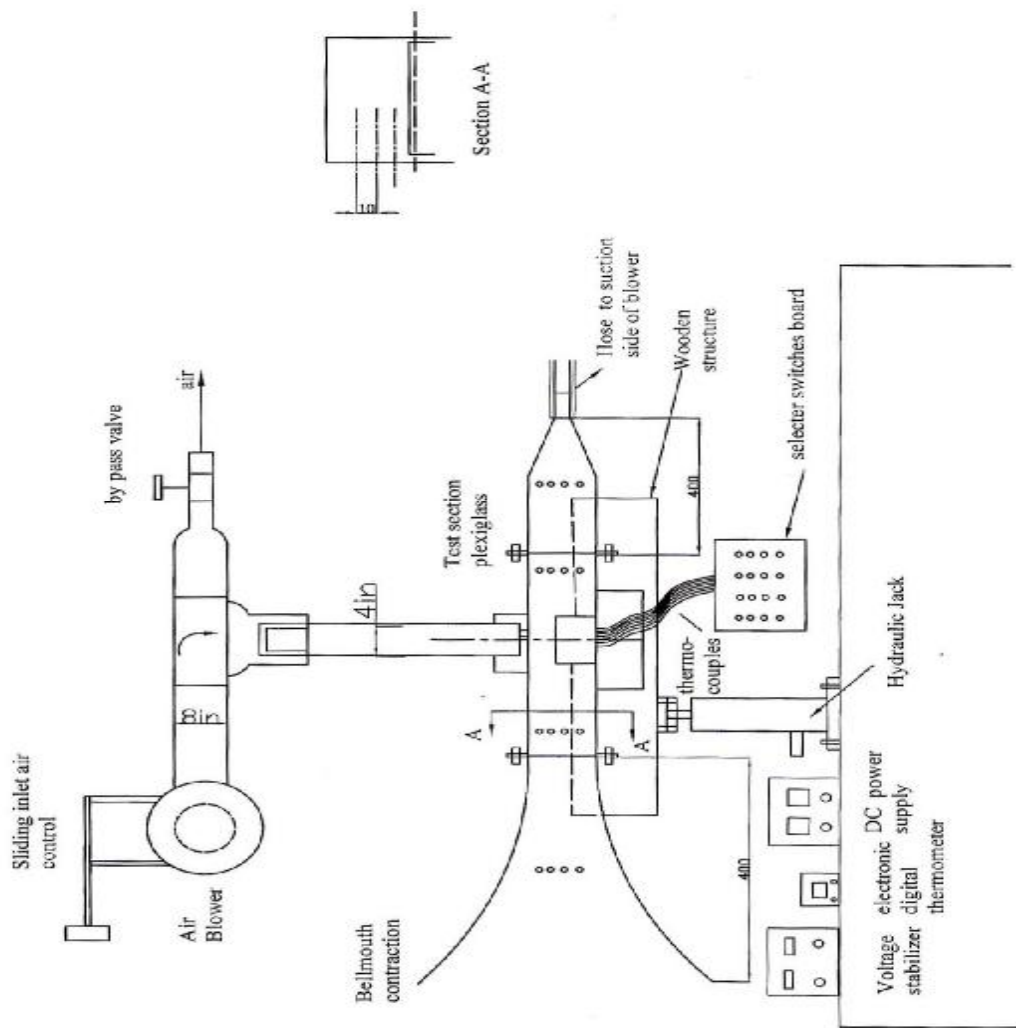


Fig. (2) Test rig details



Plate(1) Experimental Rig



Plate(2) Total Tube And Traversing Mechanism



Plate(3) Cube in The Duct

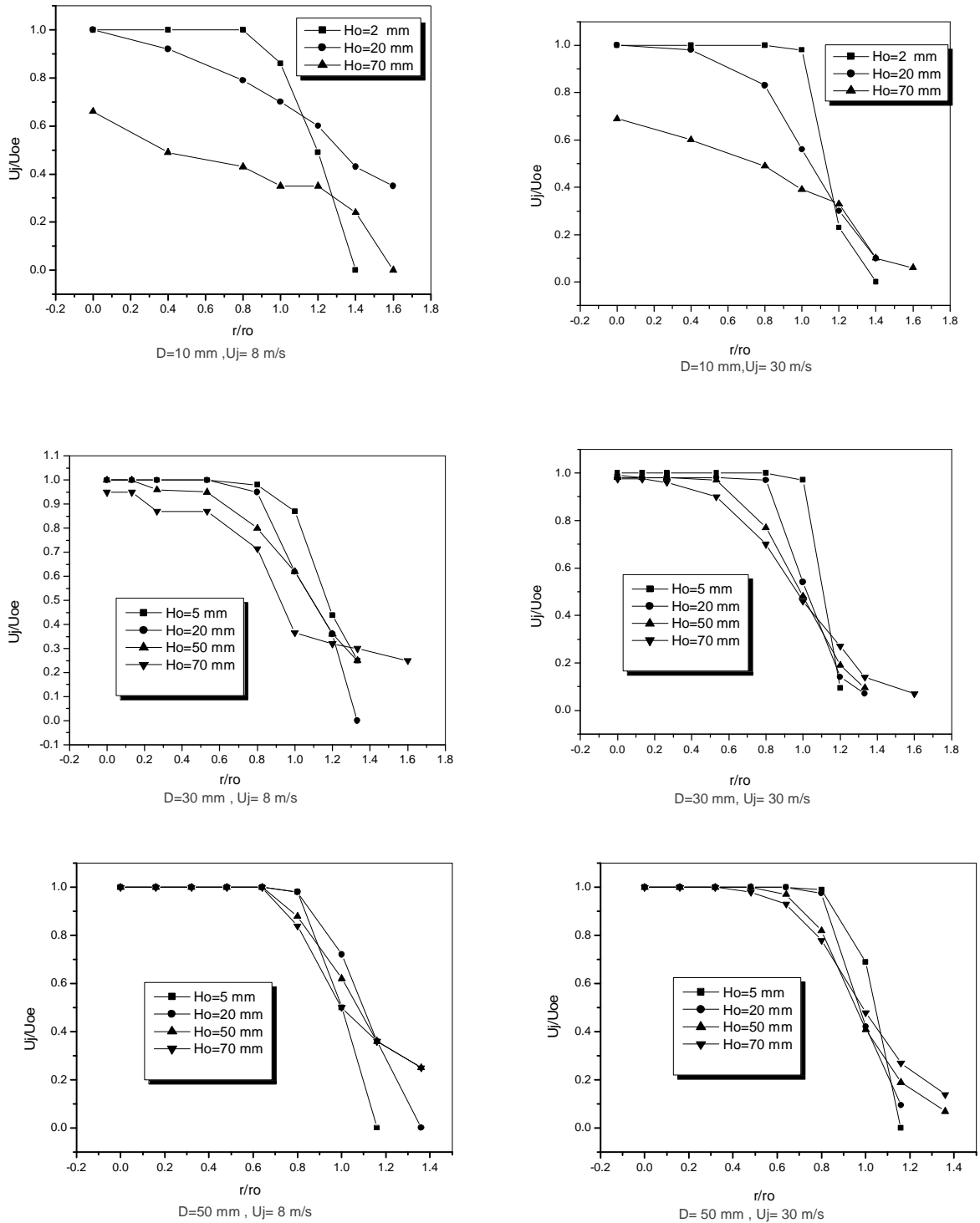


Fig.(3) Velocity Distributions At Different Jet Velocities And Axial Positions  
 $U_{oe}$ = velocity at orifice exit plane

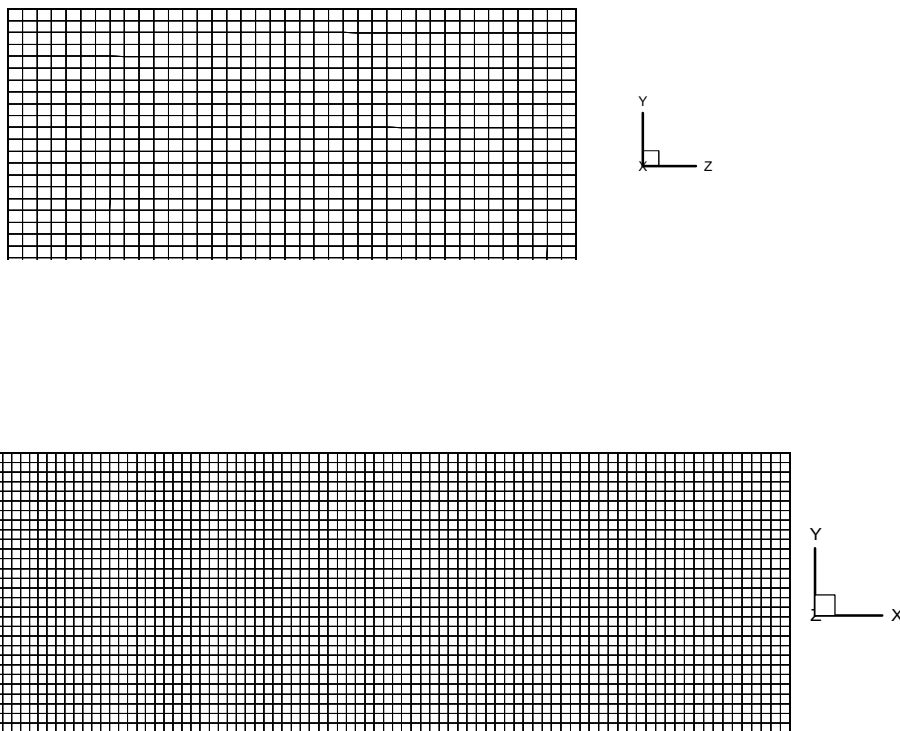


Fig. 4 Numerical Mesh

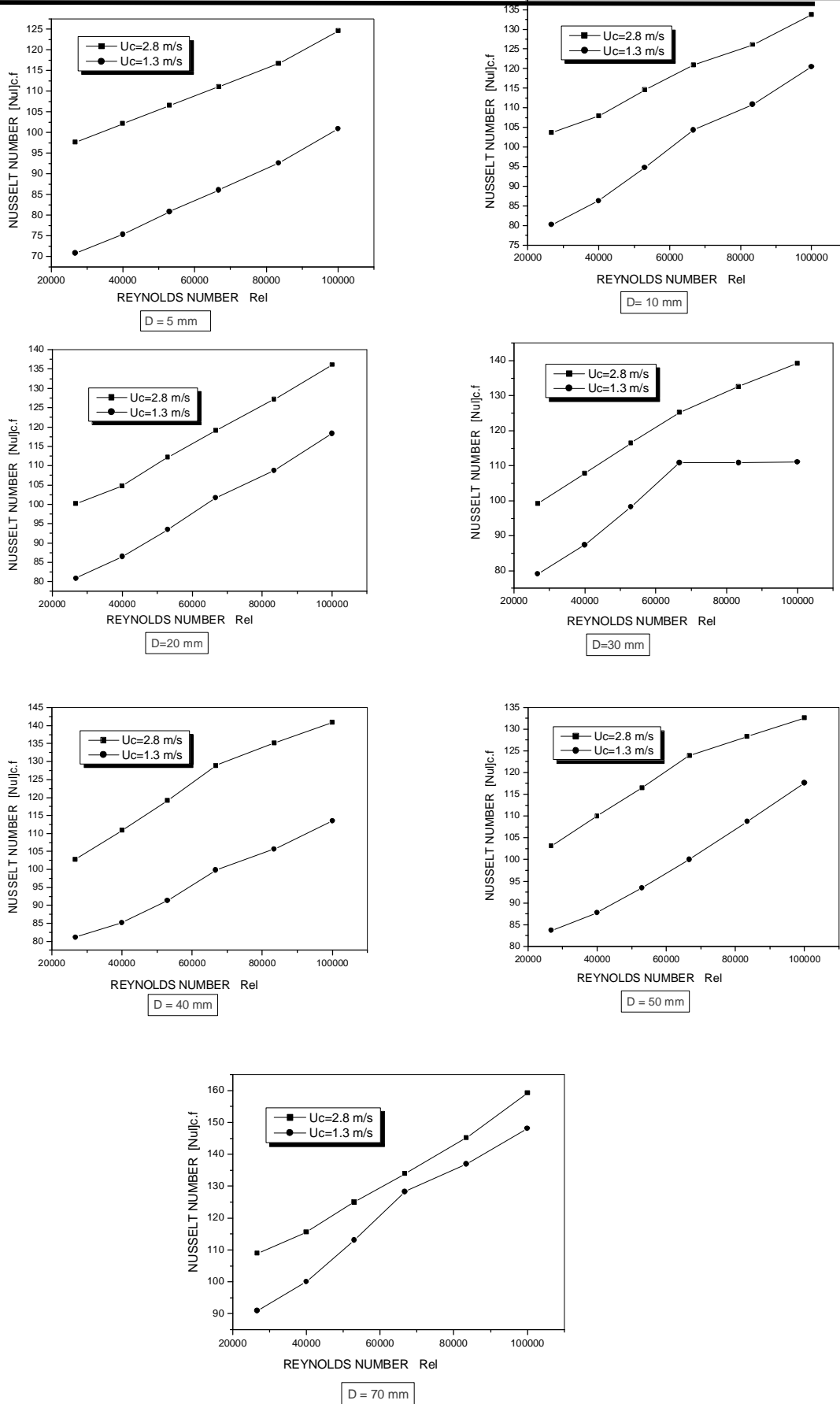


Fig. 5 Variation In Nusselt Number With Impinging Jet Reynolds Number

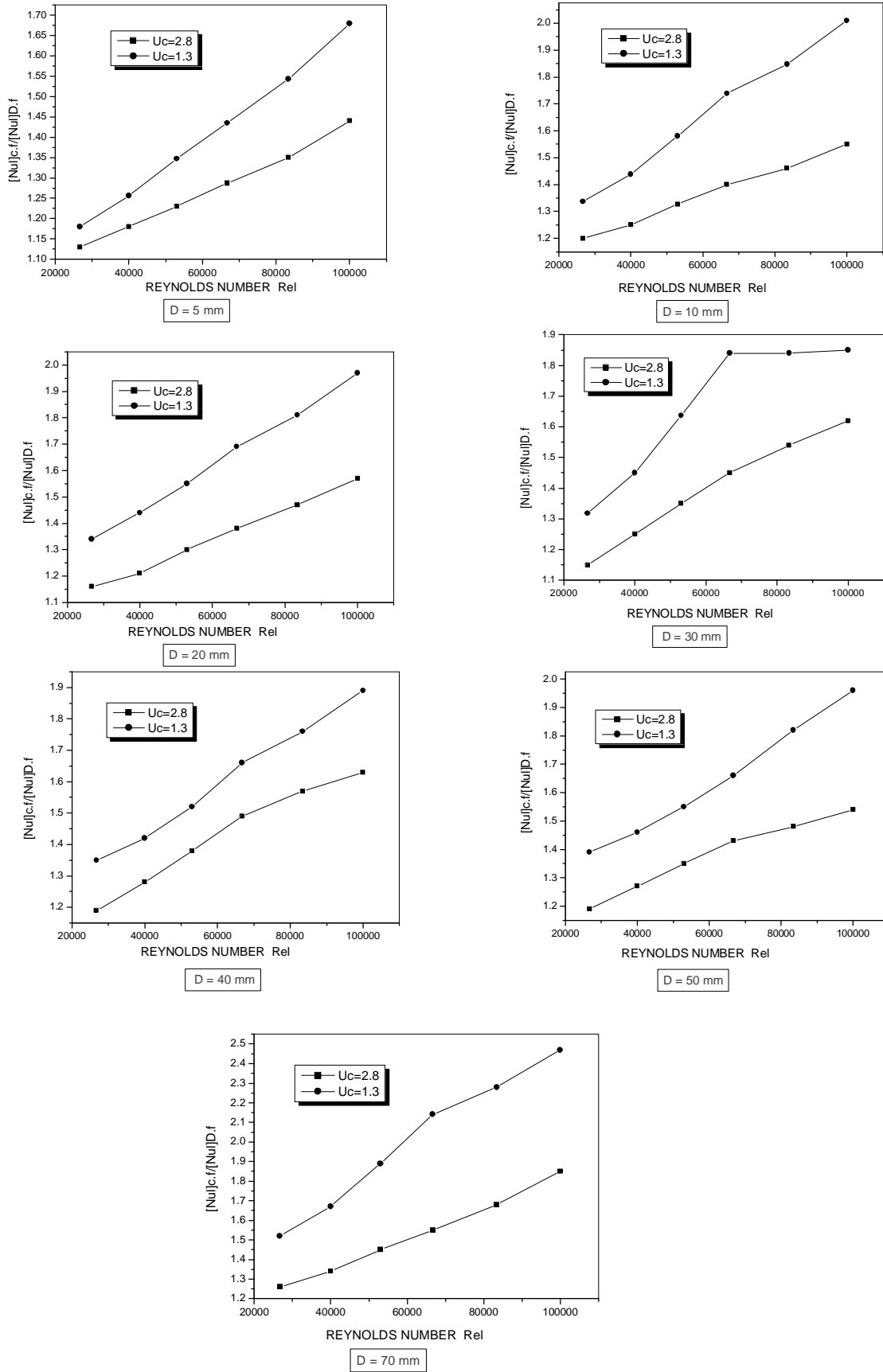


Fig. 6 Variation In Ratio Of Nusselt With Cross Flow To Nusselt For Duct Flow Only With Impinging Jet Reynolds Number ,H / L = 1.4

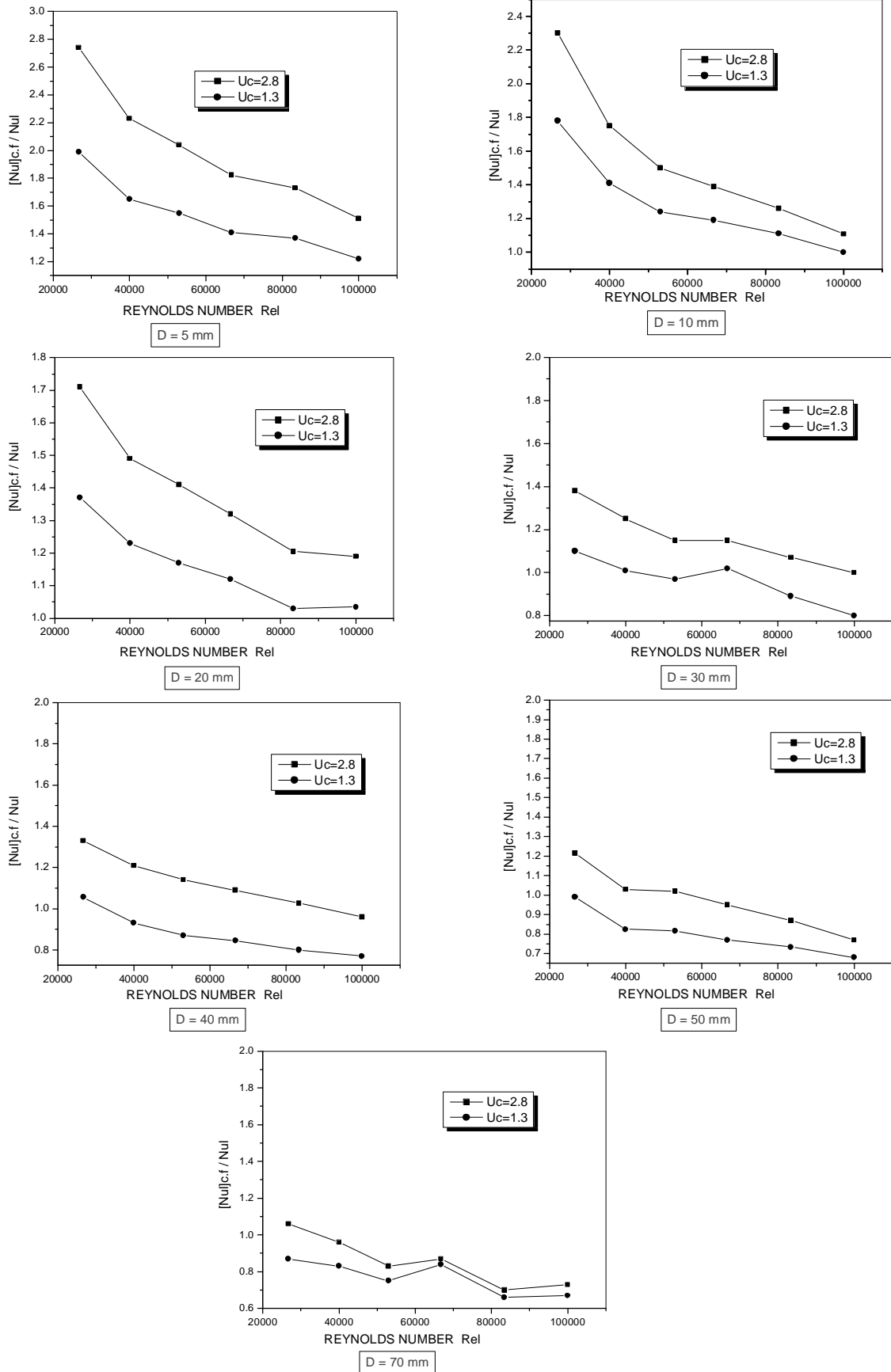


Fig. 7 Variation In The Ratio Of Nusselt With Cross Flow To Nusselt In Impingement Only With Reynolds Of Impinging Jet , H / L = 1.4

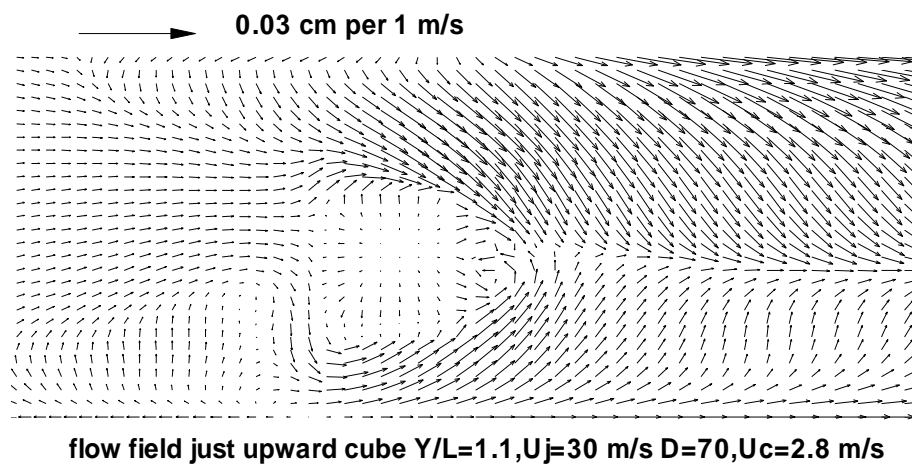
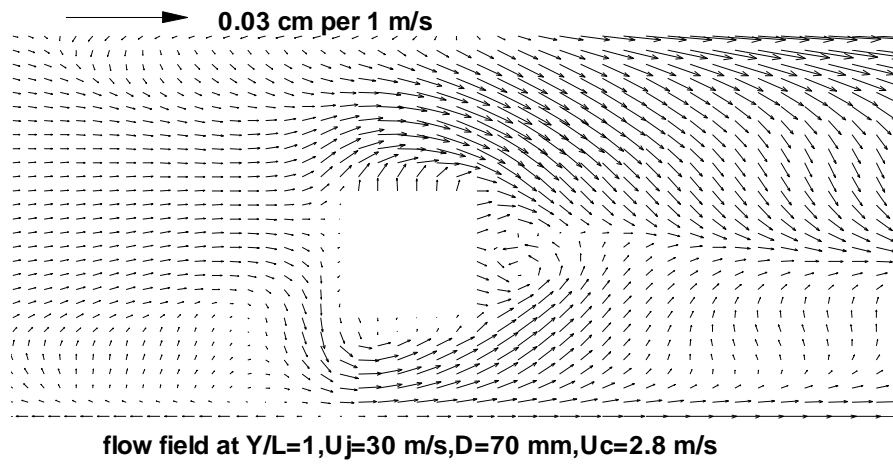
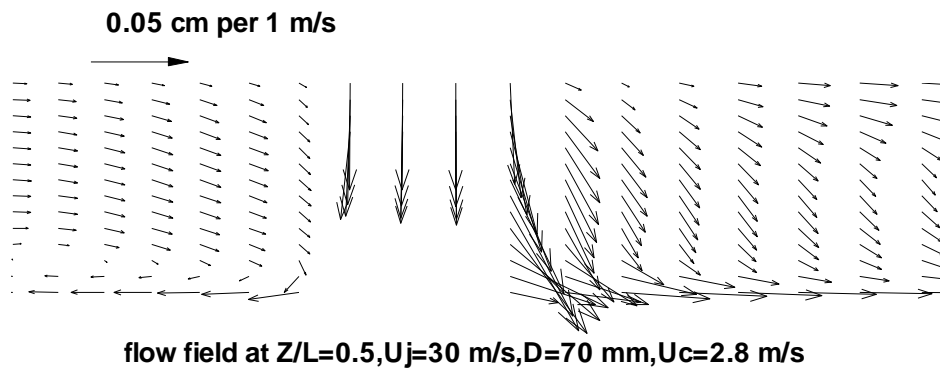


Fig. 8 Flow Field Around The Cube For Large Orifice Diameter

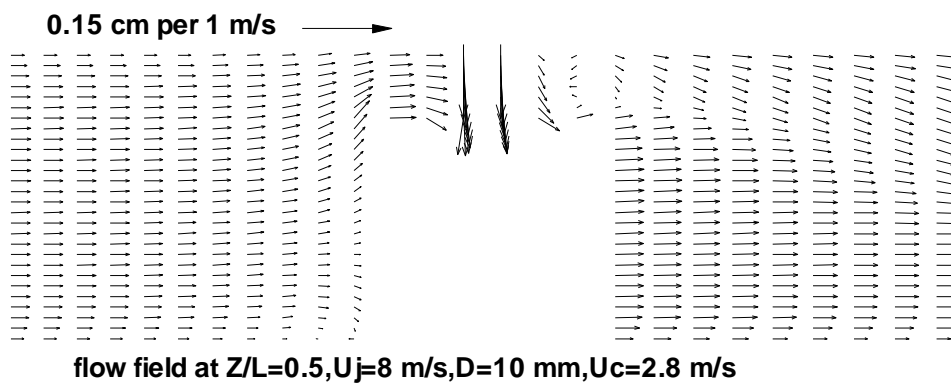


Fig. 9 Flow Field Around The Cube For Small Orifice Diameter